IEEE Access
Multidisciplinary | Rapid Review | Open Access Journal

Received 10 May 2024, accepted 13 May 2024, date of publication 16 May 2024, date of current version 28 May 2024.

Digital Object Identifier 10.1109/ACCESS.2024.3401730

RESEARCH ARTICLE

Hybrid Optimization Based Harmonic Minimization in Three Phase Multilevel Inverter With Reduced Switch Topology

MEHMET HALIL YABALAR[1] **AND ERGUN ERCELEBI**[2]
[1]Department of Electrical and Electronics Engineering, Hasan Kalyoncu University, 27010 Gaziantep, Turkey
[2]Department of Electrical and Electronics Engineering, Gaziantep University, 27310 Gaziantep, Turkey

Corresponding author: Mehmet Halil Yabalar (mehmet.yabalar@hku.edu.tr)

ABSTRACT This study presents an innovative hybrid optimization approach that combines teaching-learning based optimization (TLBO) with the whale optimization algorithm (WOA) for selective harmonic elimination (SHE) technique in a modified reduced switch topology three phase multilevel inverter (MLI). The proposed topology requires fewer switches than a conventional cascaded H-bridge MLI and another reduced switch topology in a single phase MLI. Once applied to an 11-level inverter, this hybrid strategy effectively tackles the issues of harmonic reduction and total harmonic distortion (THD) on the line-to-line voltage, significantly improving the quality of the output power through the optimal determination of switching angles. The study leverages the TLBO and WOA to solve the non-linear set of equations associated with the SHE controls technique, aiming to overcome the limitations of classical methods prone to local optimal solutions and dependent on initial controlling parameters. This method has been performed in two steps, during the first step TLBO has been executed and in the next step the solutions derived from TLBO has been used as an initial guess for WOA which ensures the attainment of the precisely converged solution. By using MATLAB® /Simulink software environment, the performance of the hybrid TLBO with WOA method has been simulated and benchmarked against traditional standalone metaheuristic techniques. The simulation results reveal that proposed hybrid approach becomes advantageous in terms of SHE and output voltage quality across various modulation indices. The experimental results verified that the proposed algorithm has been validated through the implementation of a three-phase 11-level inverter. This study highlights the significant potential of the hybrid optimization method in progressing harmonic minimization techniques within the multilevel inverters.

INDEX TERMS Teaching-learning based optimization (TLBO), whale optimization algorithm (WOA), selective harmonic elimination (SHE), reduced switch topology, multilevel inverter (MLI), total harmonic distortion (THD), modulation index.

I. INTRODUCTION

The vast proliferation of renewable energy technologies in recent years has created a vital need for innovative power conversion systems capable of transforming the electrical output from these sources into forms suitable for various types of loads [1], [2]. Among the power electronic devices available for such conversions, inverters stand out due to their ability to convert direct current (DC) power into alternating current (AC) with desired electrical characteristics [3]. This

The associate editor coordinating the review of this manuscript and approving it for publication was Rui Li.

phenomenon has significantly boosted the development of power electronic converter topology, particularly the MLIs since their discovery in 1975 [4]. Multilevel inverters (MLIs), specific type of inverters, have been at the forefront of technological advancement thanks to their capacity to generate a staircase output waveform synthesized at different voltage levels [5]. This output is mainly controlled by the accurate angle switching of the MLI power switching devices [6]. Known for their superior electromagnetic compatibility, high power quality, low switching losses, and reduced total harmonic distortion, so MLIs are commonly used use in industrial drivers, compensators, medium and high voltage inverters, as well as interfaces to renewable energy systems [5], [6]. One distinct advantage of MLIs is the use of separate DC sources, which proves highly beneficial for applications in fuel cells and photovoltaic arrays [4]. Further categorization of MLIs yields three primary configurations emerge: cascaded H-bridge, diode clamped, and capacitor clamped inverters. Among these, cascaded H-bridge inverters are noted for their structure of series connected H-bridge cells, where the sum of each cell's voltage is utilized to generate the desired output waveform [7], [8].

Despite the advancements in MLI design and structure, a continuous effort is in progress to reduce the harmonic content of MLIs [9]. Harmonic reduction, an essential aspect of an MLI's operation, largely depends on the modulation strategy chosen to control the inverter [10]. On the other hand, SHE [10], [11], [12] is a pulsed width modulation (PWM) control strategy aimed at suppressing low-order harmonics by determining the angles to control the switching sequence of the MLI power semiconductor devices [14], [15]. However, the search for an efficient and effective algorithm to solve every optimization problem in engineering and research fields always remains as a complex endeavour [16].

Among the variants of MLI, the Cascaded H-Bridge Multilevel Inverter (CHBMLI) stands out for its modular and simple structure [3]. The number of levels in CHBMLI is defined by the expression (2s+1) where s represents the number of single-phase full-bridge inverters controlled with the use of either high or low-frequency PWM techniques [7]. However, the use of high frequency switching techniques in CHBMLI can result in power losses, attributed to the numerous switching devices involved [14], [15]. To mitigate this issue, the Selective Harmonic Elimination Pulse Width Modulation (SHEPWM) method, a low-frequency modulation strategy has been used to eliminate undesired lower harmonics effectively [10].

Despite the growing prominence of SHEPWM, solving the transcendental equations required by these methods become a daunting task due to their complexities [16], [17]. This necessitates the development of fast and efficient algorithms capable of providing solutions [18]. Current methods used for solving the SHEPWM problem can be categorized into three main types: numerical methods (NMs), algebraic methods (AMs), and evolutionary algorithms (EAs) [19], [20].

In NMs, the Newton Raphson (NR) technique is utilized for solving SHE equations, offering precise and promising solutions [21]. However, these require an initial guess and may fall into local optima, risking sub-optimal outcomes.

AMs like the method of resultant theory has been discussed for optimized switching angles [22], not requiring initial guesses unlike numerical methods. However, their increased complexity and computational needs at higher inverter levels limit their use in advanced harmonic elimination.

The search for optimization solutions has led to the development of numerous EAs [23]. However, despite their benefits, most of them fail in ensuring a balance between exploration and exploitation, which is primarily vital for effective convergence of optimization [24]. Consequently, the need for algorithms that provide a global solution rather than focusing on one specific region has become increasingly prominent [25].

Considering the challenges posed by the non-linear equations associated with the SHEPWM formulation, a variety of iterative, stochastics, and metaheuristics methods have been utilized [24], [25], [26], [27], [28], [29]. In the recent algorithms including the Modified Dingo Optimization Algorithm (mDOA) [28], Black Window Optimization Algorithm (BWOA) [32], Grey Wolf Optimization Algorithm (GWOA) [28], Jumping Spider Optimization Algorithm (JSOA) [19], Modified Grey Wolf Optimization Algorithm (MGWOA) [33], Mexican Axolotl Optimization (MAO) [34], Chaos Game Optimization (CGO) [35], Coot Bird Algorithm (COOT) [36], Golden Eagle Optimizer (GEO) [37], and Harris Hawks Optimization (HHO) [38] have gained significant favour due to their proficiency in finding local optima and circumventing stagnation points [30], [31], [32], [33], [34], [35]. Despite the success of individual metaheuristics methods like the Teaching-Learning Based Optimization (TLBO), Whale Optimization Algorithm (WOA), and others, none of them are free of limitations and constraints [45]. For instance, these methods might provide optimal results for one specific application while failing to find the global optimum in other applications [46].

While WOA excels in exploration, it may suffer from excessive exploration and insufficient exploitation, leading to suboptimal results in certain scenarios. To address this limitation, it has been combined the strengths of TLBO and WOA to create a hybrid optimization algorithm that capitalizes on their complementary characteristics. In this context, the necessity for a hybrid approach becomes inevitable, which integrates different algorithms to harness their respective strengths while reducing their limitations [47].

Thus, this paper introduces a hybrid optimization methodology incorporating the TLBO and the WOA for SHE in a three-phase 11-level MLI with modified reduced switch topology [48]. This hybrid method has been implemented in MATLAB® /Simulink environment and applied to experimental prototype for seeking to offer a versatile and efficient solution to the challenge of harmonic minimization in

MLIs [49]. The primary goal of this paper is to improve the output power quality on the line-to line voltage of the MLI by optimally determining the switching angles and reducing lower-order harmonics, thus enhancing the efficiency of renewable energy systems [50].

II. MATERIALS AND METHODS

This section presents the details and comparative analysis about modified reduced switch count topology with other reduced switch topology and traditional cascaded H-Bridge. Also, this section describes selective harmonic elimination method for proposed topology.

A. REDUCED SWITCH COUNT TOPOLOGY

The number of switches needed in a traditional single-phase cascaded multilevel inverter is determined by the following expression (1):

$$k = 2(l - 1) \tag{1}$$

where k represents the required number of switches and l corresponds to the number of levels in the multilevel inverter. The reduced switch topology calculates the count of switches in the single-phase multilevel inverter in accordance with (2):

$$k = l + 3 \tag{2}$$

Fig. 1(a) presents the design of an eleven-level MLI with a reduced switch. This inverter is linked to a cascaded basic unit that inverts the waveform alternately to achieve positive, zero, negative levels. Notably, the design eliminates the requisite for additional clamping diodes or voltage balancing capacitors by utilizing isolated DC power supplies. Clamping diodes and capacitors help in balancing the voltage across each level of the inverter unless isolated DC power supplies used.

Fig. 1(b) shows the design of an 11-level MLI with a modified reduced switch. This design has two switches less. The number of switches needed in a modified reduced switch topology is determined by the following expression (3):

$$k = l + 1 \tag{3}$$

Furthermore, it also allows for adjustable output voltage levels. Switching losses are minimized by activating and deactivating the switching devices only once in each cycle. During the time interval $0 < t < (T/2)$, switches S'_1, S'_2 are simultaneously ON, generating the positive half of the output voltage waveform V_L. Conversely, in the interval $(T/2) < t < T$, the turning ON of switches S'_3, S'_4 results in the negative half of the output voltage waveform -V_L. The output phase voltage in this proposed topology is characterized by (4):

$$l = 2s + 1 \tag{4}$$

where l signifies the quantity of levels and s represents the requisite quantity of DC sources. In a standard cascaded MLI setup, the quantity of DC voltage sources is needed to match the number of output phase voltages. Fig. 2 presents a comparative analysis of the number of switches required in a conventional cascaded MLI against the number of switches required in the proposed topology. Fig. 2 also shows that the proposed topology requires fewer switches to achieve l level voltages in the output. This is a great advantage in terms of a reduction in both the installation space and the quantity of gate drivers needed [51]. For instance, the generation of a single-phase output voltage with $l = 11$ levels: the proposed topology necessitates the use of 12 switches, whereas a conventional cascaded H-bridge multilevel inverter would require 20 switches and other reduced switch topology would require 14 switches.

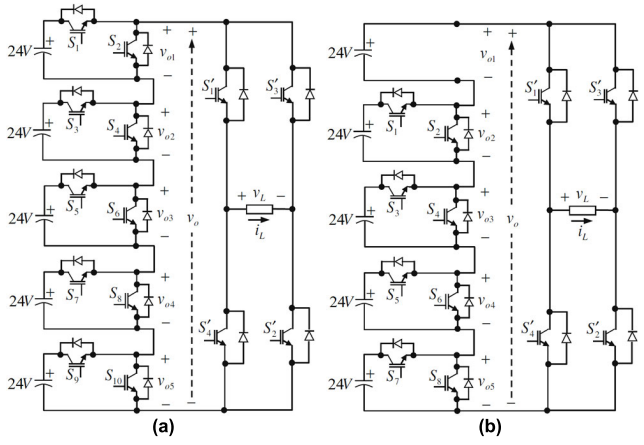

FIGURE 1. (a) Reduced switch cascaded MLI. (b) Modified reduced switch cascaded MLI.

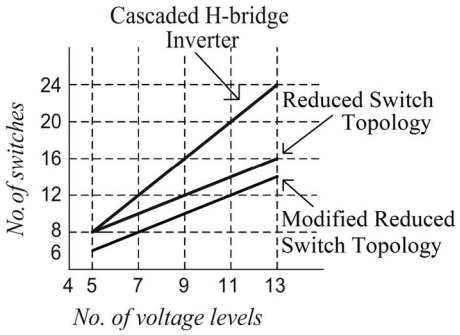

FIGURE 2. Switch counts versus output voltage levels.

MLIs make use of variety of modulation methods, broadly divided into two categories based on their switching frequencies as high or low frequency values. High frequency switching approaches including space vector pulse width modulation (SVPWM) and sinusoidal pulse width modulation (SPWM), typically require multiple commutating semiconductor switches throughout each cycle of the output voltage waveform.

On the other hand, low switching frequency schemes including SHE, synchronous optimal pulse width modulation (SOP), and space vector control (SVC) [52], typically involve

only one or two commutations per cycle. The primary benefits of low frequency switching schemes are their minimal switching losses, reduced need for filtering components, and absence of harmonic interference. These advantages make these techniques particularly well-suited for high-voltage applications [11].

In this study, low frequency switching has been applied with selective harmonic elimination method for less switching losses. The fundamental frequency and switching frequency are 50 Hz.

B. SELECTIVE HARMONIC ELIMINATION METHOD

In the design of cascaded H-bridge inverters, the staircase-like voltage output is derived from the cumulative addition of each DC source voltage (V_{dc}) across individual H-bridge cells (m), with the count of these cells (m) equating to the number of sources (s). This design establishes a relationship between the number of levels (n) and sources, expressed mathematically as $2s + 1$. Fig. 3 demonstrates a behavioural comparison between an idealized single-phase sine voltage waveform ($f(t)_V$) and the corresponding staircase voltage output of a multilevel inverter over a period (T). In this setup, the peak phase voltage matches sV_{dc} voltage, and the defined angles, which are calculated for quarter-wave symmetry, adhere to the following criteria:

$$0^\circ \leq \alpha_1 \leq \alpha_2 \leq \ldots \leq \alpha_{(S-1)} \leq \alpha_S \leq 90^\circ \tag{5}$$

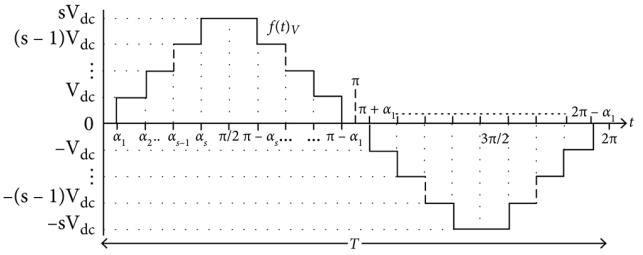

FIGURE 3. Phase voltage output of the MLI staircase.

Utilizing Fourier analysis [14], on the MLI staircase output depicted in Fig. 3 can be characterized in the following (6):

$$f(t)_V = \begin{cases} \dfrac{4V_{dc}}{n\pi}\left[cos(n\alpha_1) + \ldots + cos(n\alpha_n)\right], & for\ odd\ n \\ 0, & for\ even\ n. \end{cases} \tag{6}$$

SHE focuses on removing low-order harmonics while maintaining the fundamental component at a specified amplitude. In a three-phase connected system similar the one treated in this study; the triple harmonic contents are naturally nullified on the line-to-line voltage due to the implementation of a balanced three-phase system [53], [54], [55]. Consequently, (6) is solved to exclude the fifth, seventh, eleventh, and thirteenth order harmonics, ensuring that the amplitude of the fundamental component remains constant at M. For this reason, (6) can be reformulated as expressed in (7):

$$\begin{aligned} cos(\alpha_1) + cos(\alpha_2) + \ldots + cos(\alpha_5) &= M \\ cos(5\alpha_1) + cos(5\alpha_2) + \ldots + cos(5\alpha_5) &= 0 \\ cos(7\alpha_1) + cos(7\alpha_2) + \ldots + cos(7\alpha_5) &= 0 \\ cos(11\alpha_1) + cos(11\alpha_2) + \ldots + cos(11\alpha_5) &= 0 \\ cos(13\alpha_1) + cos(13\alpha_2) + \ldots + cos(13\alpha_5) &= 0 \end{aligned} \tag{7}$$

where $M = (V_1)/(4sV_{dc}\pi)$ is known as the modulation index within the range of $0 < M \leq 1$ and V_1 represents the desired fundamental component [46]. Under the constraints outlined in (5), (7) can be reformulated as an optimization problem [14], [56] in (8):

$$\begin{aligned} &minf\ (\alpha_1, \alpha_2, \alpha_3, \alpha_4, \alpha_5) \\ &= \left[\sum_{i=1}^{5} cos(\alpha_i) - M\right]^2 + \left[\sum_{i=1}^{5} cos(5\alpha_i)\right]^2 \\ &\quad + \left[\sum_{i=1}^{5} cos(7\alpha_i)\right]^2 + \left[\sum_{i=1}^{5} cos(11\alpha_i)\right]^2 \\ &\quad + \left[\sum_{i=1}^{5} cos(13\alpha_i)\right]^2. \end{aligned} \tag{8}$$

Upon presenting the definition of the objective function or fitness function, and before introducing the Hybrid TLBO-WOA in detail in the next section, the states of staircase voltage have been shown in Fig. 4. All steps in Fig. 3 have been described as switches ON or OFF in Table 1. Fig. 4(I) and (vii) are zero-state. Fig. 4(ii)-(vi) are positive cycle and Fig. 4(viii)-(xii) are negative cycle of output.

TABLE 1. Switching table of the proposed multilevel inverter.

#	Output	S_1	S_3	S_5	S_7	S_2	S_4	S_6	S_8	S'_1	S'_2	S'_3	S'_4
i	0	0	0	0	0	0	0	0	0	0	0	0	0
ii	V_{dc}	0	0	0	0	1	1	1	1	1	1	0	0
iii	$2V_{dc}$	1	0	0	0	0	1	1	1	1	1	0	0
iv	$3V_{dc}$	1	1	0	0	0	0	1	1	1	1	0	0
v	$4V_{dc}$	1	1	1	0	0	0	0	1	1	1	0	0
vi	$5V_{dc}$	1	1	1	1	0	0	0	0	1	1	0	0
viii	0	0	0	0	0	0	0	0	0	0	0	0	0
vii	$-V_{dc}$	0	0	0	0	1	1	1	1	0	0	1	1
ix	$-2V_{dc}$	1	0	0	0	0	1	1	1	0	0	1	1
x	$-3V_{dc}$	1	1	0	0	0	0	1	1	0	0	1	1
xi	$-4V_{dc}$	1	1	1	0	0	0	0	1	0	0	1	1
xii	$-5V_{dc}$	1	1	1	1	0	0	0	0	0	0	1	1

III. OVERVIEW OF THE PROPOSED HYBRID OPTIMIZATION ALGORITHM

In this section, TLBO, WOA and hybrid optimization method are properly presented. Proposed hybrid optimization algorithm uniquely merges two different TLBO and WOA metaheuristic techniques. A comprehensive analysis of the

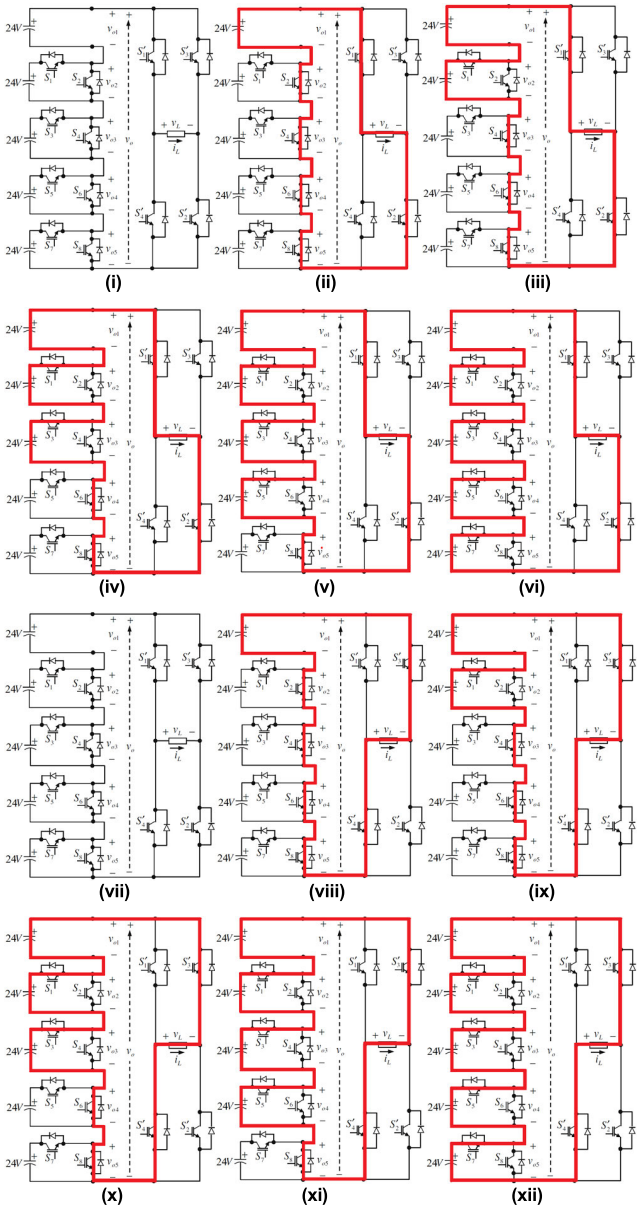

FIGURE 4. Different switching states of the proposed multilevel inverter in positive half cycle and negative half cycle.

algorithm, including its fundamental components, has been described.

A. TEACHING-LEARNING-BASED OPTIMIZATION

The TLBO, functioning as a class-based optimization method, mimics the instructional and learning dynamics found in a classroom environment. It utilizes interactions between teachers and students to enhance solution quality. This algorithm unfolds in two distinct stages: the Teacher Phase and the Learner Phase. During the Teacher Phase, the optimal solution, referred to as the 'teacher,' imparts its knowledge to the rest of the solutions, termed 'students,' within the group. The goal of this exchange is to elevate the over-all solution quality by leveraging the teacher's experience and insight. Subsequently, in the Learner Phase, the students engage in peer-to-peer learning, promoting both collaborative discovery and exploration [57].

The process of the TLBO algorithm is graphically depicted in Fig. 5. The flowchart demonstrates the process where a user-generated population undergoes a design phase, involving setting variables and termination criteria, and the calculation of other parameters like each variable's average value to determine the optimal solution. Iteration commences to find a superior solution, which, upon meeting established criteria, is adopted as the new optimum, or the search continues for an improved solution. This involves randomly selecting two solutions and keeping the better one for comparison with the previously determined best solution to decide if it should replace the existing 'teacher' solution. This process repeats until fulfilment of the completion criteria, culminating in the reporting of the finest solution achieved through these iterations.

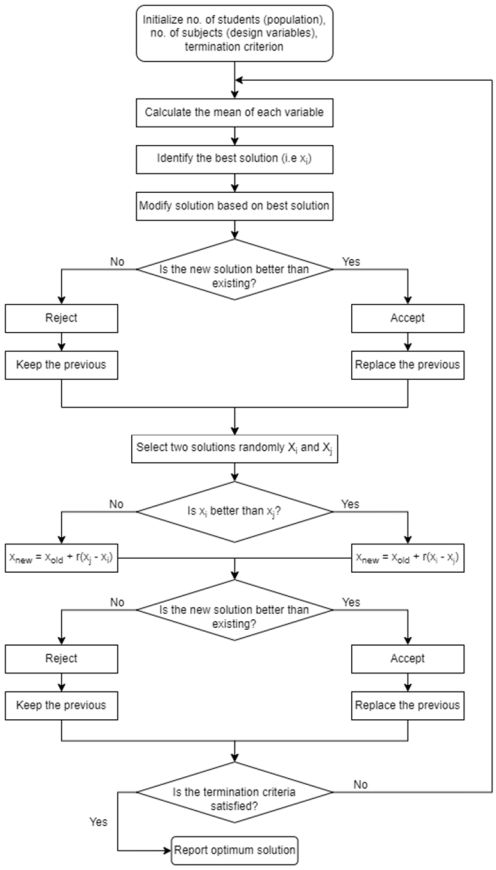

FIGURE 5. TLBO-algorithm flowchart.

One of the key strengths of TLBO is its simplicity; it only necessitates the population size and problem dimensions as its parameters. This algorithm excels in balancing exploration and exploitation, ensuring an extensive search across the solution space while effectively utilizing areas with potential. However, in certain cases, the exploration capabilities of TLBO may not be sufficient to achieve the most favourable

results then the inclusion of another metaheuristic algorithm is prompted to boost its performance [58].

B. WHALE OPTIMIZATION ALGORITHM

WOA is a nature-inspired algorithm primarily inspired by the hunting behaviour of humpback whales. Whales exhibit an impressive ability to locate and capture their prey using unique strategies such as spiral path movement and encircling behaviour. These traits make WOA well-suited for global optimization tasks, as the algorithm mimics the whales' hunting process to explore the search space efficiently [46]. The processes in the WOA algorithm are graphically depicted in Fig 6.

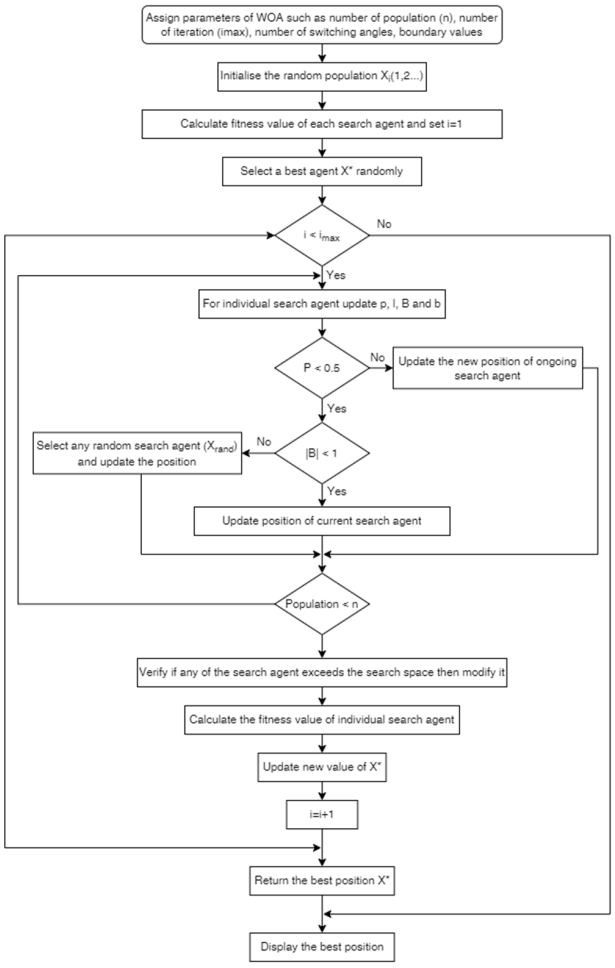

FIGURE 6. WOA-algorithm flowchart.

Although WOA is highly effective in exploration, it can sometimes be prone to over-exploration and inadequate exploitation, which might result in suboptimal outcomes under specific conditions [56].

C. PROPOSED HYBRID OPTIMIZATION ALGORITHM: TLBO-WOA

Population-based algorithms work with a set of candidate solutions by using a random search strategy. This multiple search process generally allows them to quickly reach the region where the global optimum is located. However, since these algorithms have highly probability-based search strategies, it may generally take a long time to find the optimum solution in their region. On the other hand, iterative-based algorithms generally work on a single solution candidate. With this serial structure, iterative-based algorithms can generally find the best global optimum of the search problem in a shorter-time than population-based algorithms. In this study, hybridization of TLBO and WOA algorithms is proposed in order to eliminate the above-mentioned disadvantage of population-based algorithms and increase their performance by providing serial structure. Thus, the attributes of both the TLBO and WOA are synergized in a hybrid optimization algorithm, leveraging their combined strengths for more balanced and effective results.

Proposed hybrid algorithm, named TLBO-WOA, leverages the interaction-based learning of TLBO and the hunting mechanism of WOA to achieve a balanced exploration and exploitation strategy. Our objective in merging these two algorithms is to amplify their collective efficiency and address the specific limitations each one possesses individually. The hybrid optimization algorithm is performed in two stages. In first stage, TLBO is executed, then the solution obtained from TLBO algorithm run is used as an initial solution for WOA algorithm in second stage. Thus, an iterative-based structure has been obtained by using the TLBO and WOA algorithms together. Furthermore, TLBO-WOA hybrid algorithm is also explained meticulously, and the flowchart for hybrid algorithm is shown in Fig. 7.

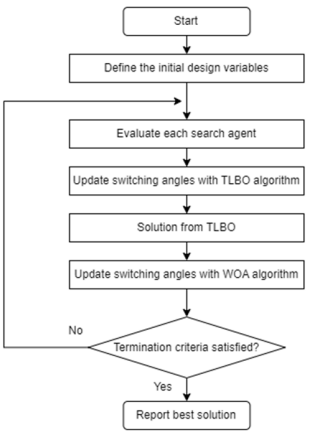

FIGURE 7. Hybrid TLBO-WOA algorithm flowchart.

In the TLBO-WOA algorithm, the Teacher Phase from TLBO plays a crucial role in spreading knowledge from the optimal solution, known as the 'teacher,' to the remaining solutions, referred as 'students,' within the population. This exchange of knowledge al-lows the students to learn from the teacher's experiences and improves their solutions. Subsequently, the Learner Phase facilitates cooperative learning and exploration among the students, allowing them to interact and exchange information. The pseudo code of the TLBO-WOA is described below.

The proposed hybrid TLBO-WOA algorithm's primary objective is to minimize THD in a three-phase eleven-level MLI. By optimizing the switching angles of the MLI, the algorithm aims to significantly reduce lower-order harmonics, thereby enhancing the power quality of the MLI. In accordance with this purpose, the switching angles are optimized in the first stage of the proposed TLBO-WOA by TLBO algorithm and then optimized switching angles solutions are improved by WOA algorithm. This process has been repeated as iterative based until termination criterion is met. So, the optimum switching angles values has been obtained by the proposed TLBO-WOA algorithm compared with the benchmark TLBO and WOA algorithms.

Pseudo Code of Hybrid TLBO-WOA

Begin procedure
Set the generation number, T = 0
Initialize N (number of students) and D (dimension)
Generation of initial students and evaluate them
while termination criterion is not satisfied **do**
  Choose the best student as $x_{teacher}$
  Calculate the mean x_{mean} of all students
  for each student x_i
    $T_F = round\,[1 + rand(0, 1)]$
    Update the student according to $x_{i,new} = x_{i,old} + rand \cdot (x_{teacher} - T_F \cdot x_{mean})$
    Evaluate the new student $x_{i,new}$
    Accept $x_{i,new}$ if it is better than the old one $x_{i,old}$
    (Teacher Phase)
    Randomly select another student x_j which is different from x_i
    Update the learner according to $x_{i,new} = \begin{cases} x_{i,old} + rand \cdot (x_i - x_j), \text{if } f(x_i) \le f(x_i) \\ x_{i,old} + rand \cdot (x_j - x_i), \text{if } f(x_i) > f(x_i) \end{cases}$
    Evaluate the new learner $x_{i,new}$
    Accept $x_{i,new}$ if it is better than the old one $x_{i,old}$
    (Learner Phase)
  end for
  Set the whales population according to the best students of TLBO
  Calculate the fitness of each search agent X^*.
  while $i < i_{max}$
    Calculate the value of a
    for each search agent
      if $p < 0.5$ then
        if $|A| < 1$ then $X(t+1) = X^*(t) - A \cdot D$
        else if $|A| \ge 1$ then $X(t+1) = X_{rand}(t) - A \cdot D''$
        end if
      else if $p \ge 0.5$ then
        $X(t+1) = D' \cdot e^{bl} \cdot \cos(2\pi l) + X^*(t)$
      end if
    end for
    Evaluate the fitness of $X(t+1)$ and update X^*
  end while
end while
Display X^*, the best optimal solution
end procedure

IV. RESULTS AND DISCUSSION

The proposed hybrid TLBO-WOA algorithm has been implemented in MATLAB to obtain the optimized switching angles for SHE of reduced switch MLI. Simulink has been utilized for the simulation of the multilevel inverter. Utilizing equal voltage sources, various voltage levels have been generated. The specifics of the simulation and optimization parameters are given with in Table 2. A Texas Instruments® -TMDS-DOCK-28335 digital signal processor has been used to implement PWM signals. Fluke-435-II Power Quality Analyzer has been used for calculation THD in experimental analysis. MLI is connected to the resistor of value 120 Ω for simulation and experimental analysis. Also, non-linear load 120 Ω and 100 mH RL load has been tested in simulation design. Furthermore, dynamic load test has been done from 120 to 40 Ω and 40 to 120 Ω in experimental design.

TABLE 2. Simulation and optimization parameters.

S. No.	Parameters/Components	Specifications	No. of Component
1.	Population Size	100	
2.	Number of Iterations	250	
3.	Number of Dimensions	5	
4.	Lower Boundary	[0° , 0° , 0° , 0° , 0°]	
5.	Upper Boundary	[90° , 90° , 90° , 90° , 90°]	
6.	Voltage Source (DC)	24 V	15
7.	Switching frequency	50 Hz	
8.	Fundamental frequency	50 Hz	
9.	R Load	R=120 Ω	Δ-connected
10.	Nonlinear Load	R= 120 Ω and L=100 mH	Δ-connected

A. SIMULATION VALIDATION

For the validation purpose, the performance of TLBO-WOA algorithm has been demonstrated with an implementation of algorithm in the MATLAB® /Simulink environment as shown in Fig. 8. Additionally, a comparative analysis has been conducted to assess the performance of TLBO-WOA against other optimization algorithms in terms of convergence solution quality.

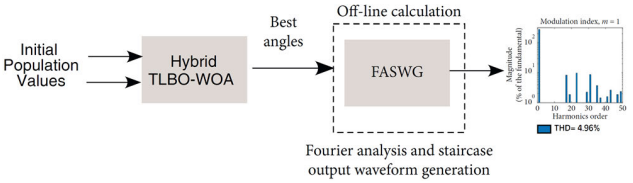

FIGURE 8. Simulink design to determine the THD for the optimal angles calculated by TLBO-WOA.

The test system is run on MATLAB® installed on an Intel® Core ™i7 10th Gen. CPU in a 2.3 GHz system with 32 GB RAM. For each test, a consistent population size of 100 and a total of 250 iterations have been conducted. The optimization process times have been calculated as follow: Hybrid TLBO-WOA at 5.81 seconds, TLBO at 5.65 seconds, and WOA at 5.53 seconds. The convergence graph of optimization algorithms has been shown in Fig. 9.

The effectiveness of the Hybrid TLBO-WOA in solving the non-linear equations associated with the SHE technique,

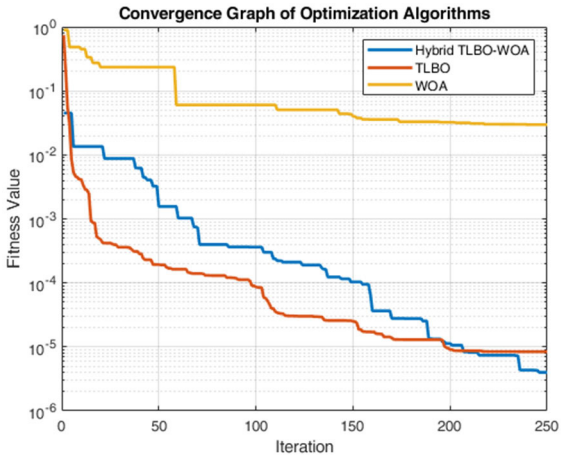

FIGURE 9. Convergence graph of optimization algorithms with population size of 100 population and 250 iterations.

three tests have been performed for each algorithm under consideration. The modulation index M considered within ranges from 0 to 1 as defined in Equation (8). Accordingly, analyses at modulation indices (m) of 0.6, 0.8, and 1 have been conducted. These values are commonly utilized in MLIs and thus have been chosen for their relevance. Results, summarized in Tables 3–6, demonstrate that the TLBO-WOA consistently achieved superior fitness across all tested modulation indices. The angles approximating the optimal solution, as determined by the TLBO-WOA, have been then applied in Fourier analysis to evaluate THD and the effective elimination of the 5th, 7th, 11th, and 13th order harmonics at the specified modulation indices. Exhibiting the most favourable outcomes, Fig. 10-12 display the Fast Fourier Transform (FFT) spectrum and line-to-line voltage output derived from the angles calculated by the TLBO-WOA, as detailed in Tables 3–5, confirming the successful minimization of the targeted low-order harmonics.

In this study, the harmonic contents in the output voltage signal of the inverter, associated with different optimization methods have been evaluated according to the IEEE-519 standard [59]. As per this standard, a minimum of 50 harmonics must be analysed to assess the quality of the inverter's output signal. The calculation of the THD percentage is conducted using (9), which is a crucial step in determining the

TABLE 3. Results of algorithms for m = 0.6.

Algorithm	Switching Angles (in degree)					THD	Fitness
	α_1	α_2	α_3	α_4	α_5		
TLBO	35.388	46.010	57.564	70.263	85.959	7.05	6.5267 x 10^{-8}
WOA	35.350	46.890	58.490	72.440	87.700	6.87	8.1700 x 10^{-5}
TLBO-WOA	35.343	46.953	58.581	72.612	87.840	6.56	5.6476 x 10^{-9}

TABLE 4. Results of algorithms for m = 0.8.

Algorithm	Switching Angles (in degree)					THD	Fitness
	α_1	α_2	α_3	α_4	α_5		
TLBO	9.729	33.372	43.353	61.220	83.691	5.56	9.1894 x 10^{-6}
WOA	33.270	44.500	52.910	64.490	76.640	5.56	3.9300 x 10^{-2}
TLBO-WOA	9.711	33.417	43.317	61.191	83.628	5.52	5.8950 x 10^{-6}

TABLE 5. Results of algorithms for m = 1.0.

Algorithm	Switching Angles (in degree)					THD	Fitness
	α_1	α_2	α_3	α_4	α_5		
TLBO	7.848	19.332	29.628	47.646	63.189	5.01	1.2657 x 10^{-5}
WOA	4.190	20.290	22.120	41.970	61.150	6.90	3.9300 x 10^{-2}
TLBO-WOA	7.821	19.359	29.574	47.610	63.198	4.96	7.8095 x 10^{-6}

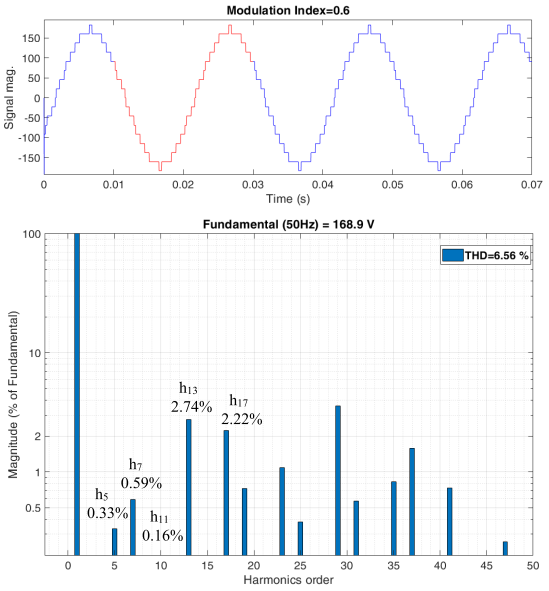

FIGURE 10. FFT analysis results of line-to-line voltage output by Hybrid TLBO-WOA in Table 1-3 with R-Load 120 Ω, modulation index = 0.6.

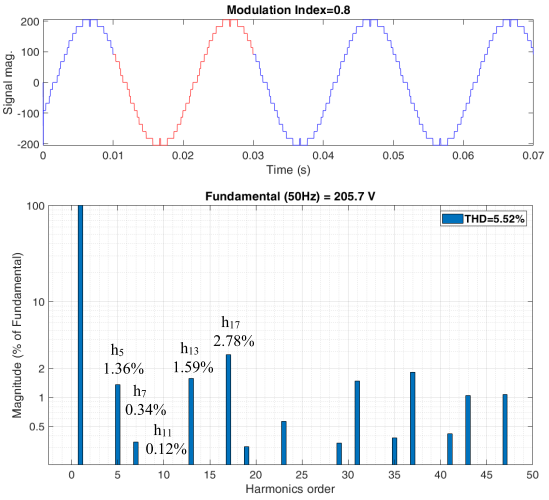

FIGURE 11. FFT analysis results of line-to-line voltage output by Hybrid TLBO-WOA in Table 1-3 with R-Load 120 Ω, modulation index = 0.8.

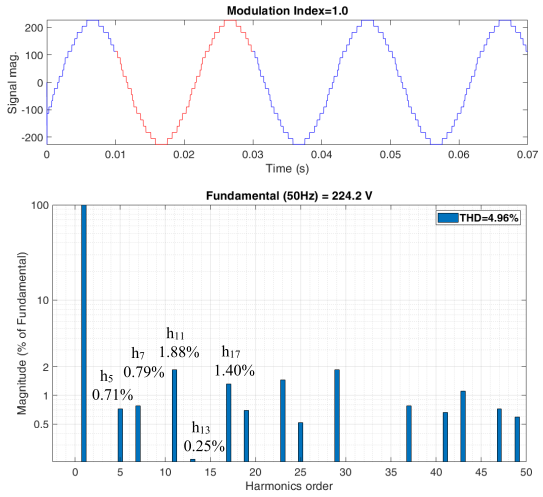

FIGURE 12. FFT analysis results of line-to-line voltage output by Hybrid TLBO-WOA in Table 1-3 with R-Load 120 Ω, modulation index = 1.0.

signal quality.

$$\%THD = \left(\frac{\sqrt{\sum_{n=1,3,5\ldots}^{50} V_n^2}}{V_1} \right) \cdot 100 \qquad (9)$$

where n represents the order of the odd harmonics (1, 3, 5, 7,…,49), V_1 is the amplitude of the first harmonic, which is the fundamental voltage, and V_n is as defined in (6).

Fig. 13 shows the output voltage and current of 120 Ω R load. Fig. 14 and Fig. 15 display FFT and output line voltage

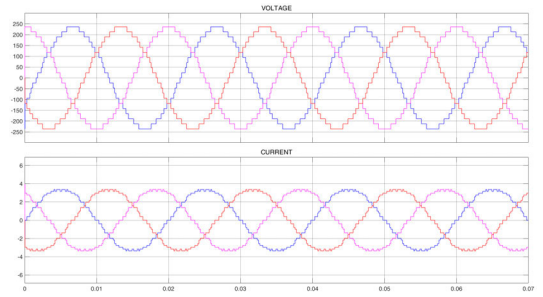

FIGURE 13. Output voltage and current of three-phase system with Δ-connected R load 120 Ω.

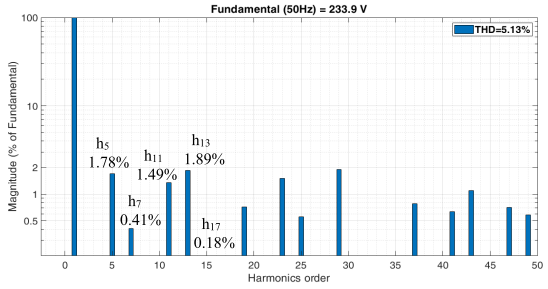

FIGURE 14. FFT spectrum of line-to-line voltage with RL load R = 120 Ω, L = 100 mH, modulation index = 1.0.

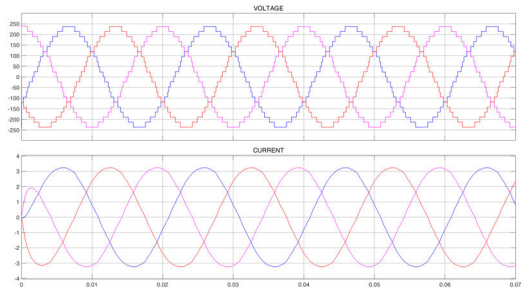

FIGURE 15. Output waveform of line-to-line voltage and current with RL load 120 Ω, 100 mH, modulation index = 1.0.

and current of 120 Ω −100 mH RL load, respectively. THD value is 5.13% for non-linear load.

Fig. 16 illustrates the switching angles from Table 6, approximating the optimal values, computed via the Hybrid TLBO-WOA for various modulation indices.

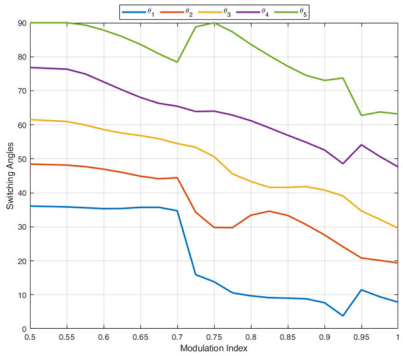

FIGURE 16. Optimized switching angles as a function of the modulation indices from 0.5 to 1.0.

TABLE 6. Results of TLBO-WOA with different modulation indices.

Modulation Index	Switching Angles (in degree)					THD	Fitness
	α_1	α_2	α_3	α_4	α_5		
0.5	36.099	48.438	58.581	61.533	90.000	10.62	5.1112×10^{-2}
0.55	35.856	48.150	60.966	76.365	90.000	8.91	1.7276×10^{-3}
0.6	35.343	46.953	58.581	72.612	87.840	6.73	5.6476×10^{-9}
0.65	35.730	44.883	56.826	68.049	83.619	6.41	4.8950×10^{-8}
0.7	34.722	44.442	54.504	65.457	78.408	6.12	2.8120×10^{-4}
0.75	15.948	34.308	53.379	63.900	88.776	5.82	1.6110×10^{-5}
0.8	9.711	33.417	43.317	61.191	83.628	5.52	5.8950×10^{-6}
0.85	9.027	33.354	41.598	56.925	77.211	5.47	1.8599×10^{-7}
0.9	7.686	27.603	40.797	52.587	73.044	5.38	3.9907×10^{-6}
0.95	11.475	20.835	34.677	54.126	62.757	5.12	2.8957×10^{-3}
1.0	7.821	19.359	29.574	47.610	63.198	4.96	7.8095×10^{-6}

Fig. 17 displays the gate signals of switches for the time interval of 50 ms. SA1, SA2, SA3, SA4, SA5, SA6, SA7, SA8, MA1, MA2, MA3, and MA4 are the gate signals for the first of the three-phase system shown in Fig. 1(b) signals S_1, S_2, S_3, S_4, S_5, S_6, S_7, S_8, S'_1, S'_2, S'_3, and S'_4 respectively. The other gate signals for the second and third

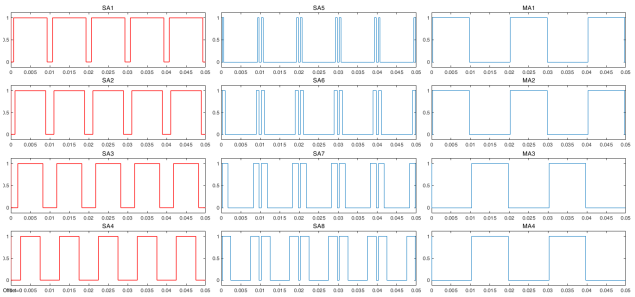

FIGURE 17. Gate signals of 11-level reduced switch MLI on Figure 1(b) simulation results.

of the three-phase systems 120° and 240° shifted according to reference signals A, respectively.

B. EXPERIMENTAL VERIFICATION

A laboratory prototype has been developed to verify the performance of the proposed TLBO-WOA optimized reduced switch 11-level three-phase MLI. The block diagram of the hardware setup is shown in Fig. 18. The parameters used in the experiment have been listed in Table 7. A Texas Instruments®-TMDS-DOCK-28335 digital signal processor has been used to implement PWM signals. Fluke-435-II Power Quality Analyzer has been used for calculation THD in experimental analysis. Logic analyzer has been used for showing gate signals of MLI.

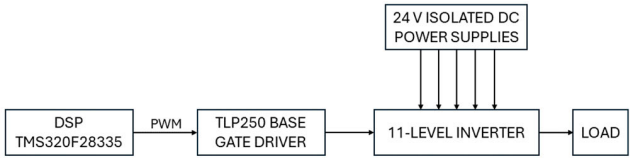

FIGURE 18. Block diagram of the hardware setup.

TABLE 7. Components used for experiment.

S. No.	Parameters/Components	Specifications	No. of Component
1.	Isolated DC power supply	24 V	15
2.	MOSFET	IRFB4227	36
3.	Gate Driver	TLP250	36
4.	DSP	TMS320F28335 (TI)	1
5.	Load	120 Ω, Δ connected	3

The photograph of hardware setup and experimental setup are shown in Fig. 19 and Fig. 20, respectively. Using isolated DC power supply is critical to designing to avoid short-circuit on common point. Fuses have been used to protect circuit board and power supplies from overload and short-circuit case.

Fig. 21 illustrates the experimental results of gate signals from logic analyzer for single phase power board. Also, Fig. 22-24 display experimental line-to-line voltage output and the FFT spectrum for modulation index 0.6, 0.8, and 1.0, respectively.

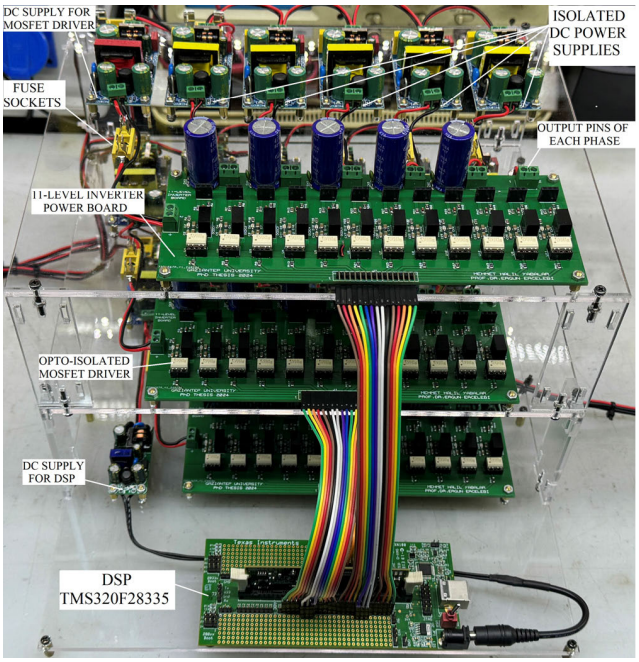

FIGURE 19. Photograph of the hardware setup.

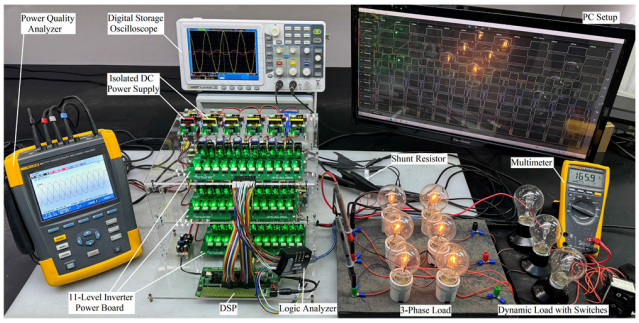

FIGURE 20. Photograph of the experimental setup.

Experimental line-to-line voltage results show that 125.54 V_{RMS} and 6.6% THD, 152.16 V_{RMS} and 5.8% THD, 165.98 V_{RMS} and 4.9% THD for modulation index 0.6, 0.8, and 1.0, respectively. It has been clear seen that oscilloscope view of line-to-line voltage 166 V_{RMS} and current 1.957 A of line with shunt resistor 0.1 Ω on Fig 25. Also, the multimeter shows the line-to-line voltage which is 165.9 V_{RMS}.

C. DYNAMIC PERFORMANCE OF THE SYSTEM

The dynamic performance of the system is validated through experimentation. The load resistance has been changed from 120 to 40 Ω to verify the dynamic behaviour. It can be observed from Fig. 26(a) that due to a decrease in load resistance, the output current increases from 1.957 to 5.871 A. Also, it can be seen from Fig. 26(b) that due to an increase in load resistance, the output current decreases from 5.871 to 1.957 A. However, the output voltage remains at 165 V. Hence, the load change does not have any effect on the output voltage.

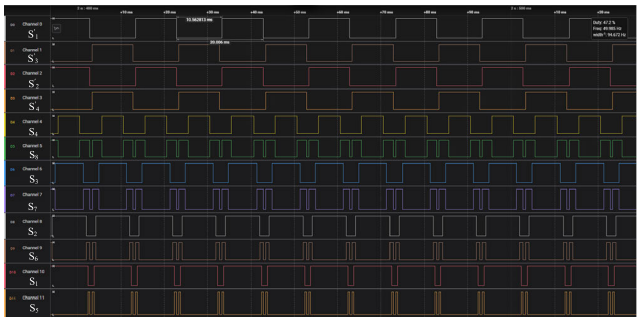

FIGURE 21. Gate signals of 11-level reduced switch MLI for experimental results of Fig. 1(b).

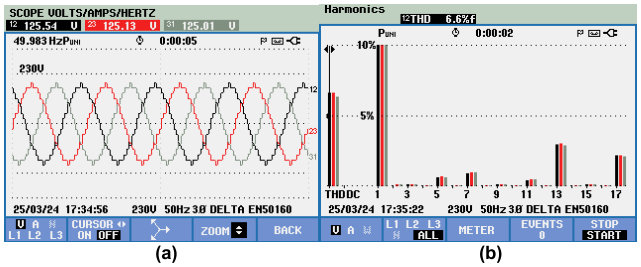

(a) (b)

FIGURE 22. Experimental results (a) line-to-line voltage for three-phase (b) FFT spectrum for modulation index 0.6 with 120 Ω load.

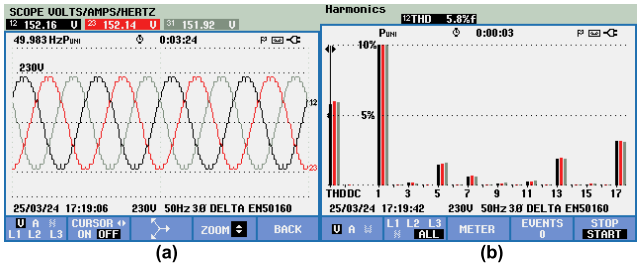

(a) (b)

FIGURE 23. Experimental results (a) line-to-line voltage for three-phase (b) FFT spectrum for modulation index 0.8 with 120 Ω load.

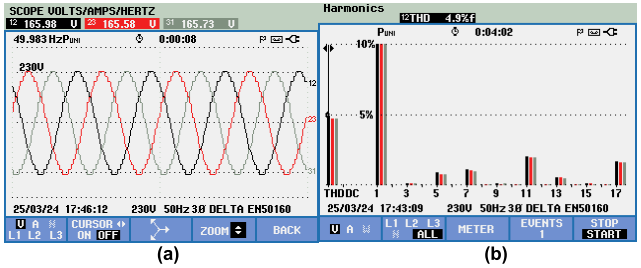

(a) (b)

FIGURE 24. Experimental results (a) line-to-line voltage for three-phase (b) FFT spectrum for modulation index 1.0 with 120 Ω load.

D. COMPARASION OF RESULTS

Several algorithms including the Modified Dingo Optimization Algorithm (mDOA) [28], Black Window Optimization Algorithm (BWOA) [32], Grey Wolf Optimization Algorithm (GWOA) [28], Jumping Spider Optimization Algorithm (JSOA) [19], Modified Grey Wolf Optimization Algorithm (MGWOA) [33], Mexican Axolotl Optimization (MAO) [34], Chaos Game Optimization (CGO) [35], Coot Bird Algorithm (COOT) [36], Golden Eagle Optimizer (GEO) [37], and Harris Hawks Optimization (HHO) [38] have been selected for a detailed comparative analysis in Table 8-10. The nearly optimal angles derived from these algorithms have been input into a Simulink to generate the

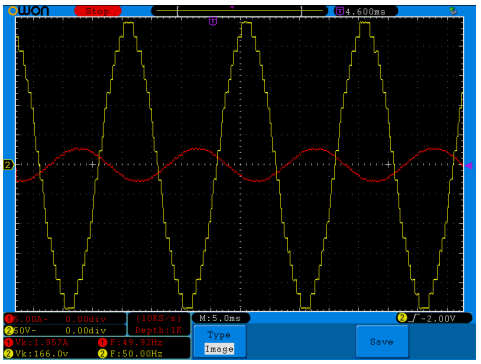

FIGURE 25. Oscilloscope results of line-to-line voltage (yellow line) and current measurement with shunt resistor 0.1 Ω (red line).

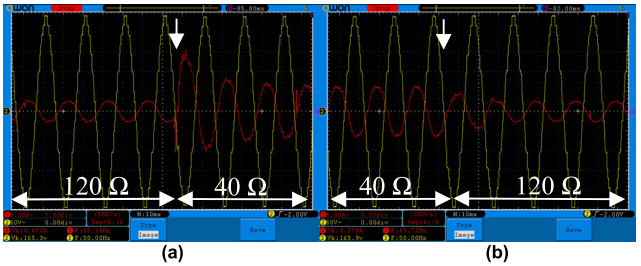

(a) (b)

FIGURE 26. Dynamic load change (a) from 120 Ω to 40 Ω, (b) from 40 Ω to 120 Ω with switch.

TABLE 8. Results of comparative analysis for the selective harmonic elimination problem (m = 0.6).

Algorithm	Switching Angles (in degree)					THD	Fitness
	α_1	α_2	α_3	α_4	α_5		
mDOA	35.420	46.940	58.570	72.670	87.850	6.79	4.1500×10^{-27}
BWOA	35.440	46.950	58.580	72.610	87.860	6.82	4.1900×10^{-27}
GWOA	35.290	46.800	58.450	72.460	87.740	6.87	2.7800×10^{-4}
WOA	35.350	46.890	58.490	72.440	87.700	6.87	8.1700×10^{-5}
TLBO	35.388	46.010	57.564	70.263	85.959	7.05	6.5267×10^{-8}
TLBO-WOA	**35.343**	**46.953**	**58.581**	**72.612**	**87.840**	**6.56**	$\mathbf{5.6476 \times 10^{-9}}$

TABLE 9. Results of comparative analysis for the selective harmonic elimination problem (m = 0.8).

Algorithm	Switching Angles (in degree)					THD	Fitness
	α_1	α_2	α_3	α_4	α_5		
mDOA	9.710	33.420	43.280	61.160	83.590	5.62	3.0100×10^{-29}
BWOA	9.700	33.430	43.300	61.180	83.600	5.63	3.0500×10^{-29}
GWOA	10.320	31.830	44.740	62.230	85.650	6.73	3.3700×10^{-3}
WOA	33.270	44.500	52.910	64.490	76.640	5.56	3.9300×10^{-2}
TLBO	9.729	33.372	43.353	61.220	83.691	5.56	9.1894×10^{-6}
TLBO-WOA	**9.711**	**33.417**	**43.317**	**61.191**	**83.628**	**5.52**	$\mathbf{5.8950 \times 10^{-6}}$

TABLE 10. Results of comparative analysis for the selective harmonic elimination problem (m = 1.0).

Algorithm	Switching Angles (in degree)					THD	Fitness
	α_1	α_2	α_3	α_4	α_5		
mDOA	7.840	19.370	29.630	47.660	62.900	5.01	1.2200×10^{-28}
BWOA	7.860	19.370	29.650	47.680	63.210	5.01	1.2900×10^{-28}
GWOA	0.490	14.740	25.610	40.570	89.160	5.71	16.0400×10^{-2}
JSOA	7.860	19.360	29.650	47.680	63.200	5.01	3.4900×10^{-31}
MGWOA	0.490	14.740	25.610	40.570	89.160	5.71	16.0400×10^{-2}
MAO	9.670	22.370	33.040	51.910	64.630	5.26	3.6400×10^{-1}
CGO	13.250	26.370	45.930	46.050	87.220	13.99	9.7600×10^{-2}
COOT	7.970	19.460	29.790	47.740	63.200	5.04	3.4300×10^{-4}
GEO	8.620	10.600	38.760	76.590	83.170	14.83	4.6400×10^{-1}
HHO	8.160	19.500	30.150	48.210	63.350	5.16	2.6900×10^{-4}
WOA	4.190	20.290	22.120	41.970	61.150	6.90	3.9300×10^{-2}
TLBO	7.848	19.332	29.628	47.646	63.189	5.01	1.2657×10^{-5}
TLBO-WOA	**7.821**	**19.359**	**29.574**	**47.610**	**63.198**	**4.96**	**7.8095×10^{-6}**

TABLE 11. Results of comparative analysis for simulation and experimental with harmonic contents.

Index	Analysis	% h_5	% h_7	% h_{11}	% h_{13}	THD	V_{RMS}
m=0.6	Simulation	0.33	0.59	0.16	2.74	6.56%	126.81 V
	Experiment	0.34	0.60	0.17	2.76	6.60%	125.54 V
m=0.8	Simulation	1.36	0.34	0.12	1.59	5.52%	153.69 V
	Experiment	1.38	0.34	0.13	1.61	5.80%	152.16 V
m=1.0	Simulation	0.71	0.79	1.88	0.25	4.96%	167.64 V
	Experiment	0.72	0.80	1.90	1.41	4.90%	165.98 V

staircase output waveform. Subsequently, THD has been calculated, and a Fourier spectrum has been produced to verify the effective minimize of undesirable low-order harmonics.

According to THD and fitness values presented in Table 10, the JSOA achieves the best fitness values, however Hybrid TLBO-WOA's THD result is better than others. This is related with other harmonics up to 50^{th} shown in Fig. 12. Also, Table 11 shows the results of comparative analysis for simulation and experimental. It can be understood that nearly %1 difference between simulation and experimental results.

V. CONCLUSION

This research has focused on using the Hybrid TLBO-WOA method to reduce THD on the line-to-line voltage in a modified reduced switch MLI topology. The proposed topology requires the use of 12 switches for 11-level inverter, whereas a conventional cascaded H-bridge MLI would require 20 switches and other reduced switch topology would require 14 switches in single phase inverter. The performance of the study has been verified by both simulation and experimental prototype. A comparative analysis of calculated THD values, using these optimized angles and those reported in existing literature using various optimization methods, revealed that the TLBO-WOA algorithm achieves favourably lower THD in the 11-level inverter than most reported methods. Proposed algorithm for lowering THD values is found to be 3.96% compared to the other algorithms. This algorithm's standout characteristic is its lack of parameter requirements, necessitating from users only the initial inputs of population size, design variables, maximum iteration count, and the objective function. The examination of the Hybrid TLBO-WOA algorithm demonstrates its efficiency in optimization, capability of effectively handling various types of problems with or without constraints. Its user-friendly nature, stemming from no need for tuning control parameters, making it highly adaptable to a wide array of problem scenarios. The main concluding remarks are as follows:

- The study under dynamic load conditions performed excellently.
- In each modulation indices, the hybrid algorithm provided better THD value.
- The experimental results have been verified the simulation results with %1 difference.
- Both simulation and experimental findings demonstrate that the Hybrid TLBO-WOA successfully maintained the output voltage THD within the acceptable limits prescribed by IEEE 519 standard.

REFERENCES

[1] A. Moeed Amjad and Z. Salam, "A review of soft computing methods for harmonics elimination PWM for inverters in renewable energy conversion systems," *Renew. Sustain. Energy Rev.*, vol. 33, pp. 141–153, May 2014, doi: 10.1016/j.rser.2014.01.080.

[2] S. Chu and A. Majumdar, "Opportunities and challenges for a sustainable energy future," *Nature*, vol. 488, no. 7411, pp. 294–303, Aug. 2012, doi: 10.1038/nature11475.

[3] J. Rodriguez, L. G. Franquelo, S. Kouro, J. I. Leon, R. C. Portillo, M. A. M. Prats, and M. A. Perez, "Multilevel converters: An enabling technology for high-power applications," *Proc. IEEE*, vol. 97, no. 11, pp. 1786–1817, Nov. 2009, doi: 10.1109/jproc.2009.2030235.

[4] J. Rodriguez, J.-S. Lai, and F. Zheng Peng, "Multilevel inverters: A survey of topologies, controls, and applications," *IEEE Trans. Ind. Electron.*, vol. 49, no. 4, pp. 724–738, Aug. 2002, doi: 10.1109/TIE.2002.801052.

[5] L. Franquelo, J. Rodriguez, J. Leon, S. Kouro, R. Portillo, and M. Prats, "The age of multilevel converters arrives," *IEEE Ind. Electron. Mag.*, vol. 2, no. 2, pp. 28–39, Jun. 2008, doi: 10.1109/MIE.2008.923519.

[6] S. Kouro, M. Malinowski, K. Gopakumar, J. Pou, L. G. Franquelo, B. Wu, J. Rodriguez, M. A. Pérez, and J. I. Leon, "Recent advances and industrial applications of multilevel converters," *IEEE Trans. Ind. Electron.*, vol. 57, no. 8, pp. 2553–2580, Aug. 2010, doi: 10.1109/TIE.2010.2049719.

[7] G. Carrara, S. Gardella, M. Marchesoni, R. Salutari, and G. Sciutto, "A new multilevel PWM method: A theoretical analysis," *IEEE Trans. Power Electron.*, vol. 7, no. 3, pp. 497–505, Jul. 1992.

[8] M. Kuder, A. Kersten, J.-L. Marques-Lopez, J. Estaller, J. Buberger, F. Schwitzgebel, T. Thiringer, A. Lesnicar, R. Marquardt, T. Weyh, and R. Eckerle, "Capacitor voltage balancing of a grid-tied, cascaded multilevel converter with binary asymmetric voltage levels using an optimal one-step-ahead switching-state combination approach," *Energies*, vol. 15, no. 2, p. 575, Jan. 2022, doi: 10.3390/en15020575.

[9] S. Khomfoi and L. M. Tolbert, "Multilevel power converters," in *Power Electronics Handbook*. USA: Academic, Jan. 2007, pp. 451–482, doi: 10.1016/B978-012088479-7/50035-3.

[10] H. S. Patel and R. G. Hoft, "Generalized techniques of harmonic elimination and voltage control in thyristor inverters: Part I-harmonic elimination," *IEEE Trans. Ind. Appl.*, vol. IA-9, no. 3, pp. 310–317, May 1973, doi: 10.1109/TIA.1973.349908.

[11] M. S. A. Dahidah, G. Konstantinou, and V. G. Agelidis, "A review of multilevel selective harmonic elimination PWM: Formulations, solving algorithms, implementation and applications," *IEEE Trans. Power Electron.*, vol. 30, no. 8, pp. 4091–4106, Aug. 2015, doi: 10.1109/TPEL.2014.2355226.

[12] M. D. Siddique, S. Mekhilef, S. Padmanaban, M. A. Memon, and C. Kumar, "Single-phase step-up switched-capacitor-based multilevel inverter topology with SHEPWM," *IEEE Trans. Ind. Appl.*, vol. 57, no. 3, pp. 3107–3119, May 2021, doi: 10.1109/TIA.2020.3002182.

[13] E. Guan, P. Song, M. Ye, and B. Wu, "Selective harmonic elimination techniques for multilevel cascaded H-bridge inverters," in *Proc. Int. Conf. Power Electron. Drives Syst.*, Kuala Lumpur, Malaysia, 2005, pp. 1441–1446, doi: 10.1109/PEDS.2005.1619915.

[14] A. K. Al-Othman and T. H. Abdelhamid, "Elimination of harmonics in multilevel inverters with non-equal DC sources using PSO," *Energy Convers. Manage.*, vol. 50, no. 3, pp. 756–764, Mar. 2009, doi: 10.1016/j.enconman.2008.09.047.

[15] K. El-Naggar and T. H. Abdelhamid, "Selective harmonic elimination of new family of multilevel inverters using genetic algorithms," *Energy Convers. Manage.*, vol. 49, no. 1, pp. 89–95, Jan. 2008, doi: 10.1016/j.enconman.2007.05.014.

[16] T. Jacob and L. P. Suresh, "A review paper on the elimination of harmonics in multilevel inverters using bioinspired algorithms," in *Proc. Int. Conf. Circuit, Power Comput. Technol. (ICCPCT)*, Mar. 2016, pp. 1–8, doi: 10.1109/ICCPCT.2016.7530273.

[17] L. Cao, J. Lin, S. Chen, and Y. Ye, "Symmetrical cascaded switched-capacitor multilevel inverter based on hybrid pulse width modulation," *Energies*, vol. 14, no. 22, p. 7643, Nov. 2021, doi: 10.3390/en14227643.

[18] S. Toumi, Y. Amirat, E. Elbouchikhi, Z. Zhou, and M. Benbouzid, "Techno-economic optimal sizing design for a tidal stream turbine-battery system," *J. Mar. Sci. Eng.*, vol. 11, no. 3, p. 679, Mar. 2023, doi: 10.3390/jmse11030679.

[19] H. Peraza-Vázquez, A. Peña-Delgado, P. Ranjan, C. Barde, A. Choubey, and A. B. Morales-Cepeda, "A bio-inspired method for mathematical optimization inspired by arachnida salticidade," *Mathematics*, vol. 10, no. 1, p. 102, Dec. 2021, doi: 10.3390/math10010102.

[20] D. E. Goldberg, *Genetic Algorithms in Search, Optimization and Machine Learning*. Boston, MA, USA: Addison-Wesley Longman, 1989.

[21] J. Sun, S. Beineke, and H. Grotstollen, "Optimal PWM based on real-time solution of harmonic elimination equations," *IEEE Trans. Power Electron.*, vol. 11, no. 4, pp. 612–621, Jul. 1996. [Online]. Available: https://api.semanticscholar.org/CorpusID:110857674

[22] J. N. Chiasson, L. M. Tolbert, K. J. McKenzie, and Z. Du, "A complete solution to the harmonic elimination problem," *IEEE Trans. Power Electron.*, vol. 19, no. 2, pp. 491–499, Mar. 2004, doi: 10.1109/tpel.2003.823207.

[23] J. H. Holland, *Adaptation in Natural and Artificial Systems: An Introductory Analysis With Applications To Biology, Control, and Artificial Intelligence*. Ann Arbor, MI, USA: University of Michigan Press, 1975.

[24] M. Clerc and J. Kennedy, "The particle swarm–explosion, stability, and convergence in a multidimensional complex space," *IEEE Trans. Evol. Comput.*, vol. 6, no. 1, pp. 58–73, 2002, doi: 10.1109/4235.985692.

[25] X. Yao, Y. Liu, and G. Lin, "Evolutionary programming made faster," *IEEE Trans. Evol. Comput.*, vol. 3, no. 2, pp. 82–102, Jul. 1999, doi: 10.1109/4235.771163.

[26] D. Karaboga and B. Basturk, "A powerful and efficient algorithm for numerical function optimization: Artificial bee colony (ABC) algorithm," *J. Global Optim.*, vol. 39, no. 3, pp. 459–471, Oct. 2007, doi: 10.1007/s10898-007-9149-x.

[27] M. R. Hussan, M. I. Sarwar, A. Sarwar, M. Tariq, S. Ahmad, A. S. N. Mohamed, I. A. Khan, and M. M. A. Khan, "Aquila optimization based harmonic elimination in a modified H-bridge inverter," *Sustainability*, vol. 14, no. 2, p. 929, Jan. 2022, doi: 10.3390/su14020929.

[28] J. H. Almazán-Covarrubias, H. Peraza-Vázquez, A. F. Peña-Delgado, and P. M. García-Vite, "An improved dingo optimization algorithm applied to SHE-PWM modulation strategy," *Appl. Sci.*, vol. 12, no. 3, p. 992, Jan. 2022, doi: 10.3390/app12030992.

[29] N. I. Siddiqui, A. Alam, L. Quayyoom, A. Sarwar, M. Tariq, H. Vahedi, S. Ahmad, and A. S. N. Mohamed, "Artificial jellyfish search algorithm-based selective harmonic elimination in a cascaded H-bridge multilevel inverter," *Electronics*, vol. 10, no. 19, p. 2402, Oct. 2021, doi: 10.3390/electronics10192402.

[30] M. Tariq, U. Shami, M. Fakhar, S. Kashif, G. Abbas, N. Ullah, A. Mohammad, and M. Farrag, "Dragonfly algorithm-based optimization for selective harmonics elimination in cascaded H-bridge multilevel inverters with statistical comparison," *Energies*, vol. 15, no. 18, p. 6826, Sep. 2022, doi: 10.3390/en15186826.

[31] R. A. Khan, S. A. Farooqui, M. I. Sarwar, S. Ahmad, M. Tariq, A. Sarwar, M. Zaid, S. Ahmad, and A. Shah Noor Mohamed, "Archimedes optimization algorithm based selective harmonic elimination in a cascaded H-bridge multilevel inverter," *Sustainability*, vol. 14, no. 1, p. 310, Dec. 2021, doi: 10.3390/su14010310.

[32] A. F. Peña-Delgado, H. Peraza-Vázquez, J. H. Almazán-Covarrubias, N. T. Cruz, P. M. García-Vite, A. B. Morales-Cepeda, and J. M. Ramirez-Arredondo, "A novel bio-inspired algorithm applied to selective harmonic elimination in a three-phase eleven-level inverter," *Math. Problems Eng.*, vol. 2020, pp. 1–10, Dec. 2020, doi: 10.1155/2020/8856040.

[33] A. Routray, R. K. Singh, and R. Mahanty, "Harmonic reduction in hybrid cascaded multilevel inverter using modified grey wolf optimization," *IEEE Trans. Ind. Appl.*, vol. 56, no. 2, pp. 1827–1838, Mar. 2020, doi: 10.1109/TIA.2019.2957252.

[34] Y. Villuendas-Rey, J. L. Velázquez-Rodríguez, M. D. Alanis-Tamez, M.-A. Moreno-Ibarra, and C. Yáñez-Márquez, "Mexican axolotl optimization: A novel bioinspired heuristic," *Mathematics*, vol. 9, no. 7, p. 781, Apr. 2021, doi: 10.3390/math9070781.

[35] S. Talatahari and M. Azizi, "Chaos game optimization: A novel metaheuristic algorithm," *Artif. Intell. Rev.*, vol. 54, no. 2, pp. 917–1004, Feb. 2021, doi: 10.1007/s10462-020-09867-w.

[36] I. Naruei and F. Keynia, "A new optimization method based on COOT bird natural life model," *Exp. Syst. Appl.*, vol. 183, Nov. 2021, Art. no. 115352, doi: 10.1016/j.eswa.2021.115352.

[37] L. Abualigah, M. Shehab, M. Alshinwan, S. Mirjalili, and M. A. Elaziz, "Ant lion optimizer: A comprehensive survey of its variants and applications," *Arch. Comput. Methods Eng.*, vol. 28, no. 3, pp. 1397–1416, May 2021, doi: 10.1007/s11831-020-09420-6.

[38] A. A. Heidari, S. Mirjalili, H. Faris, I. Aljarah, M. Mafarja, and H. Chen, "Harris hawks optimization: Algorithm and applications," *Future Gener. Comput. Syst.*, vol. 97, pp. 849–872, Aug. 2019, doi: 10.1016/j.future.2019.02.028.

[39] Z. W. Geem, J. H. Kim, and G. V. Loganathan, "A new heuristic optimization algorithm: Harmony search," *Simulation*, vol. 76, no. 2, pp. 60–68, Feb. 2001, doi: 10.1177/003754970107600201.

[40] A. R. Lopez, O. A. López-Núñez, R. Pérez-Zúñiga, J. Gómez Radilla, M. Martínez-García, M. A. López-Osorio, G. Ortiz-Torres, M. G. Mena-Enriquez, M. Ramos-Martinez, J. C. Mixteco-Sánchez, C. A. Torres-Cantero, F. D. J. Sorcia-Vázquez, and J. Y. Rumbo-Morales, "Total harmonic distortion reduction in multilevel inverters through the utilization of the moth–flame optimization algorithm," *Appl. Sci.*, vol. 13, no. 21, p. 12060, Nov. 2023, doi: 10.3390/app132112060.

[41] S. A. Farooqui, M. M. Shees, M. F. Alsharekh, S. Alyahya, R. A. Khan, A. Sarwar, M. Islam, and S. Khan, "Crystal structure algorithm (CryStAl) based selective harmonic elimination modulation in a cascaded H-bridge multilevel inverter," *Electronics*, vol. 10, no. 24, p. 3070, Dec. 2021, doi: 10.3390/electronics10243070.

[42] S. Ürgün, H. Yiğit, and S. Mirjalili, "Investigation of recent metaheuristics based selective harmonic elimination problem for different levels of multilevel inverters," *Electronics*, vol. 12, no. 4, p. 1058, Feb. 2023, doi: 10.3390/electronics12041058.

[43] N. Riad, W. Anis, A. Elkassas, and A. E.-W. Hassan, "Three-phase multilevel inverter using selective harmonic elimination with marine predator algorithm," *Electronics*, vol. 10, no. 4, p. 374, Feb. 2021, doi: 10.3390/electronics10040374.

[44] S. Ahmad, "Electromagnetic field optimization based selective harmonic elimination in a cascaded symmetric H-bridge inverter," *Energies*, vol. 15, no. 20, p. 7682, Oct. 2022, doi: 10.3390/en15207682.

[45] R. V. Rao, V. J. Savsani, and D. P. Vakharia, "Teaching–learning-based optimization: A novel method for constrained mechanical design optimization problems," *Comput.-Aided Design*, vol. 43, no. 3, pp. 303–315, Mar. 2011, doi: 10.1016/j.cad.2010.12.015.

[46] S. Mirjalili and A. Lewis, "The whale optimization algorithm," *Adv. Eng. Softw.*, vol. 95, pp. 51–67, May 2016, doi: 10.1016/j.advengsoft.2016.01.008.

[47] X.-S. Yang, "A new metaheuristic bat-inspired algorithm," in *Nature Inspired Cooperative Strategies for Optimization (NICSO)* (Studies in Computational Intelligence). Berlin, Germany: Springer, 2010, pp. 65–74, doi: 10.1007/978-3-642-12538-6_6.

[48] K. Deep and M. Thakur, "A new mutation operator for real coded genetic algorithms," *Appl. Math. Comput.*, vol. 193, no. 1, pp. 211–230, Oct. 2007, doi: 10.1016/j.amc.2007.03.046.

[49] E. Rashedi, H. Nezamabadi-pour, and S. Saryazdi, "GSA: A gravitational search algorithm," *Inf. Sci.*, vol. 179, no. 13, pp. 2232–2248, Jun. 2009, doi: 10.1016/j.ins.2009.03.004.

[50] E. Barbie, D. Baimel, and A. Kuperman, "Analytical expression for line voltage THD of three-phase staircase modulated multilevel inverters," *Electronics*, vol. 11, no. 3, p. 364, Jan. 2022, doi: 10.3390/electronics11030364.

[51] S. D. Patil and S. G. Kadwane, "Hybrid optimization algorithm applied for selective harmonic elimination in multilevel inverter with reduced switch topology," *Microsyst. Technol.*, vol. 24, no. 8, pp. 3409–3415, Aug. 2018, doi: 10.1007/s00542-018-3720-x.

[52] A. Edpuganti and A. K. Rathore, "A survey of low switching frequency modulation techniques for medium-voltage multilevel converters," *IEEE Trans. Ind. Appl.*, vol. 51, no. 5, pp. 4212–4228, Sep. 2015, doi: 10.1109/TIA.2015.2437351.

[53] A. Kavousi, B. Vahidi, R. Salehi, M. K. Bakhshizadeh, N. Farokhnia, and S. H. Fathi, "Application of the bee algorithm for selective harmonic elimination strategy in multilevel inverters," *IEEE Trans. Power Electron.*, vol. 27, no. 4, pp. 1689–1696, Apr. 2012, doi: 10.1109/TPEL.2011.2166124.

[54] M. H. Etesami, N. Farokhnia, and S. Hamid Fathi, "Colonial competitive algorithm development toward harmonic minimization in multilevel inverters," *IEEE Trans. Ind. Informat.*, vol. 11, no. 2, pp. 459–466, Apr. 2015, doi: 10.1109/TII.2015.2402615.

[55] I. H. Shanono, N. R. H. Abdullah, and A. Muhammad, "A survey of multilevel voltage source inverter topologies, controls, and applications," *Int. J. Power Electron. Drive Syst. (IJPEDS)*, vol. 9, no. 3, p. 1186, Sep. 2018, doi: 10.11591/ijpeds.v9.i3.pp1186-1201.

[56] P. Kumar Kar, A. Priyadarshi, and S. Bhaskar Karanki, "Selective harmonics elimination using whale optimisation algorithm for a single-phase-modified source switched multilevel inverter," *IET Power Electron.*, vol. 12, no. 8, pp. 1952–1963, Jul. 2019, doi: 10.1049/iet-pel.2019.0087.

[57] K. Y. Gómez Díaz, S. E. De León Aldaco, J. Aguayo Alquicira, M. Ponce-Silva, and V. H. Olivares Peregrino, "Teaching–learning-based optimization algorithm applied in electronic engineering: A survey," *Electronics*, vol. 11, no. 21, p. 3451, Oct. 2022, doi: 10.3390/electronics11213451.

[58] K. Y. Gómez Díaz, S. E. de León Aldaco, J. A. Alquicira, and L. G. V. Valdés, "THD minimization in a seven-level multilevel inverter using the TLBO algorithm," *Eng*, vol. 4, no. 3, pp. 1761–1786, Jun. 2023, doi: 10.3390/eng4030100.

[59] *IEEE Recommended Practice and Requirements for Harmonic Control in Electric Power Systems*, Standard IEEE Std 519-2014, Piscataway, NJ, USA, 2014, pp. 1–29.

MEHMET HALIL YABALAR was born in Gaziantep, Turkey. He received the B.Sc. degree in electrical and electronics engineering from Ege University, Izmir, Turkey, in 2015, and the M.Sc. degree from Gaziantep University, Gaziantep, in 2019, where he is currently pursuing the Ph.D. degree in electrical and electronics engineering. He is also a Research Assistant with the Department of Electrical and Electronics Engineering, Hasan Kalyoncu University, Gaziantep. His research focuses on power electronics.

ERGUN ERCELEBI received the B.Sc. degree in electrical and electronics engineering from Middle East Technical University, Turkey, in 1990, and the M.Sc. and Ph.D. degrees from Gaziantep University, Gaziantep, Turkey, in 1992 and 1999, respectively. He is currently a Professor with the Electrical and Electronics Engineering Department, Gaziantep University. His research interests include communication techniques, signal processing, embedded systems software, and machine learning.